Energetic and Exergetic Performance Comparison of a Compression-Absorption System Working with NH_3-H_2O, NH_3-$LiNO_3$ and NH_3-NaSCN

J.L. Rodríguez-Muñoz[1], J.M. Belman-Flores[2,*], V. Pérez-García[2], A. Gallegos-Muñoz[2], C. Rubio-Maya[3] and S. Méndez-Díaz[4]

[1]*School of Industrial Engineering UNIDEG-SABES, University of SABES, Pénjamo, 36900, México*

[2]*Engineering Division Campus Irapuato-Salamanca, University of Guanajuato, Salamanca 36885, México*

[3]*Faculty of Mechanical Engineering, Edif. W, CU., Universidad Michoacana de San Nicolás de Hidalgo, Morelia 58030, México*

[4]*Faculty of Mechanical and Electrical Engineering, Universidad Autónoma de Nuevo León, Nuevo León 66451, México*

Abstract: The inclusion of a compressor in absorption refrigeration systems is one of the practices that are becoming more common in the refrigeration field, since a lower generation temperature is required. Among the mixtures most used and studied in refrigeration-compression cycles (CARC) are NH_3-$LiNO_3$ and NH_3-NaSCN. This is mainly due to the assumption that these two mixtures have a better energy efficiency than the conventional absorption refrigeration cycle working with NH_3-H_2O (BARC). Therefore, this work shows an energy and exergy study of a CARC cycle, in which its analysis extends to the use of the NH_3-H_2O mixture, to show the potential that presents the mixture for refrigeration and air conditions applications, as well as the advantages and disadvantages to operating in this type of configurations. The results obtained are compared with the mixtures NH_3-$LiNO_3$ and NH_3-NaSCN at different evaporation, condensation, generation temperatures and different compressor pressure ratio. The results show that the generation temperature, as well as the energetic and exergetic efficiency are strongly dependent on the compressor pressure ratio. For compression ratio values lesser than 1.6, NH_3-NaSCN mixture is energetically higher than NH_3-H_2O and NH_3-$LiNO_3$ at generation temperatures higher than 70°C. The results show the three mixtures have very similar exergetic behavior for almost all wide range of operating conditions. When the system works with *rp*=2.0, the COP of NH_3-H_2O mixture is 3.26% higher than the other two mixtures, while under the same operations conditions, the energetic behavior is very similar for the three mixtures for different generation and evaporation temperatures.

Keywords: Refrigeration, modeling, performance, absorption/compression.

1. INTRODUCTION

Nowadays, refrigeration systems are extremely important in daily life, since they allow to satisfy diverse needs in different sectors of society. Most refrigeration systems (including air conditioning) used around the world are based on vapor compression technology. However, this type of technology consumes between 15 to 30% of globally electricity produced and contributes 10% to the increasing of greenhouse gases emissions [1]. In this sense, an alternative refrigeration technology is that based on absorption. This has the advantage of presenting a lower demand of energy consumption, as well as lower greenhouse gases emissions, as a result of the type of input energy and the type of working pair. For example, Kalinowski *et al*. [2] researched the application of waste heat to reduce electricity consumption in absorption refrigeration systems. They concluded that with a Combined Cooling, Heating and Power systems, reduction of electricity consumption is achieved. Xu *et al*. [3] analyzed a serial LiBr-H_2O absorption heat pump where the waste heat recovery system was carried out. Their results show the energy recovered for the proposed configuration can save until 31.93% of the total energy supplied to the system. Yue *et al*. [4] studied a solar absorption and absorption-compression hybrid refrigeration in building cooling. They concluded this configuration has the higher cooling capacity and lower fuel consumption compared with the conventional solar/natural gas-driven absorption chiller. On a commercial level, the most typical working pairs used in absorption refrigeration systems are NH_3-H_2O and LiBr-H_2O. NH_3-H_2O is suitable for refrigeration applications, while LiBr-H_2O is commonly used in air conditioning systems. A disadvantage of NH_3-H_2O pair in the basic absorption refrigeration cycle compared to other working pairs is its lower energy efficiency, this due to the use of a rectifier. Derived from the above, several studies have focused on determining, from the energy or exergy point of view, those working pairs that contribute to achieve improvements to the basic

*Address correspondence to this author at the Engineering Division Campus Irapuato-Salamanca, University of Guanajuato, Salamanca 36885, México; Tel: 01464 6479940; Fax: +52 (464) 6479940 Ext. 2311;
E-mail: jfbelman@ugto.mx

E-ISSN: 2409-5826/19

absorption refrigeration cycle. Among the most promising working pairs are found, NH_3-$LiNO_3$ and NH_3-NaSCN. In this contest, Zhu and Gu [5] analyzed by the second law of thermodynamics an absorption system for cooling and heating application using NH_3-NaSCN as working fluid. They concluded that the COP of cooling and heating increases with the heat source temperature and decreases with the cooling water inlet temperature. An air-cooled non-adiabatic absorption refrigeration system working with NH_3-$LiNO_3$ and NH_3-NaSCN was studied by Cai *et al.* [6]. In their study, the effect of the generator, absorber outlet temperature, absorber efficiency on the energetic efficiency were discussed. The analysis results indicate that relatively high system performance can be obtained when non adiabatic absorber is applied in these systems. Cai *et al.* [7] also evaluated experimentally on the thermal performance of an air-cooled absorption refrigeration cycle with NH_3-$LiNO_3$ and NH_3-NaSCN refrigerant solutions. Their results showed that the COP of NH_3-NaSCN mixture is higher than that of NH_3-$LiNO_3$ system. Farshi *et al.* [8] made a simulation of an NH_3-$LiNO_3$ and NH_3-NaSCN absorption refrigeration cycles where various operating parameters on the performance and the possibility of crystallization in the cycles are studied. They concluded for high generator temperatures, NH_3-NaSCN cycles have better performance. In addition to the above, there are studies that have incorporated the use of a compressor to the basic absorption refrigeration cycle in order to determine the effect on the energetic efficiency of the system. In this context, the configurations commonly found in the literature are Hybrid configuration in series and Hybrid configuration in parallel [9].

In the series configuration, the compressor can be located in two zones, between the generator and the condenser, and between the evaporator and the absorber, called the compression-absorption cycle, CARC. While in the second configuration, the compressor is integrated into parallel between the absorber and the generator, also known as the resorption-compression cycle, RCAC. Emphasizing the Hybrid configuration in series, this configuration has the advantage of requiring much lower generation temperature, as well as the use of less energy compared to the conventional absorption refrigeration system. In this context, Wang *et al*. [10] studied an absorption-compression hybrid refrigeration system recovering condensation heat for the generation. Their results show the generation temperature decreases 70-80% and the primary energy efficiency can be 97.1% higher than that of conventional absorption refrigeration system. Wu *et al*. [11] conducted an experimental study of a compression-absorption system with NH_3-H_2O, which operated in heat pump mode. This configuration worked more efficiently at a lower inlet generator temperature, achieving increases of up to 94% in cooling capacity compared to the traditional heat pump.

The exergy analysis is a potential tool used to identify the sources, magnitude and location of the reversibility in energy systems [12]. Therefore, Ayou *et al*. [13] investigated a combined refrigeration and power system from the energy and exergy point of view. Their results show that this cycle is more beneficial than the conventional one, since it is flexible enough to adjust its heat source temperature requirement to produce the same cooling capacity adjusting directly the compressor pressure ratio, *rp*. Takleh and Zare [14] modeled a combined power and ejector-refrigeration cycle where a thermoelectric generator and booster compressor were incorporated. They found that the booster assisted incorporated with the thermoelectric generator has higher exergy efficiency by around 18.7% than the conventional combined power and ejector refrigeration system driven by geothermal energy. Razmi *et al*. [15] conducted an energy and exergy analysis of a hybrid absorption/refrigeration system. They concluded that with this configuration non-crystallization working range occurs at low generation temperature in comparison with single effect absorption system. Other studies have focused on evaluating the energetic performance of the compression-absorption refrigeration system, using the NH_3-$LiNO_3$ pair. For example, Ventas *et al*. [16] conducted a theoretical study of a compression-absorption cycle, in which the effect of the activation temperature as well as the compressor pressure ratio was analyzed at a fixed condensation and evaporation temperature. Their results showed that for *rp*=2.0, the activation temperature reduced to up 24°C, this in comparison to the basic absorption refrigeration cycle. Later, the authors extended their study and found that the compression-absorption system produced the refrigeration effect at activation temperatures between 57 and 70°C, where the maximum energetic efficiency of 0.5 was obtained with a compressor pressure ratio of 2.2.

According to the reviewed literature, most of the studies focus on the energy comparative study and use of NH_3-NaSCN and NH_3-$LiNO_3$ in the CARC, and the use and analysis of NH_3-H_2O in this type of systems configurations is limited. Therefore, this paper intends

to broaden the discussion of energy and exergy analysis of a compression-absorption refrigeration system in which three working pairs are compared: NH_3-H_2O, NH_3-$LiNO_3$ and NH_3-NaSCN. Besides, the study shows the operating conditions in which the best energy and exergy behaviors are obtained, and their possible operational limitations in the field of refrigeration and/or air conditioning. The study is developed for different values of evaporation, condensation and generation temperatures, as well as for different values of compressor pressure ratio. Above study has the objective of establishing that the NH_3-H_2O pair may be more appropriate than pairs NH_3-$LiNO_3$ and NH_3-NaSCN based on coefficient of performance, COP, exergetic efficiency, η_{ex} and operating conditions when implementing within a CARC cycle. In addition, the results obtained for the CARC cycle are compared with those obtained by the conventional absorption refrigeration cycle, BARC, under the same operating conditions.

2. DESCRIPTION OF THE ABSORPTION REFRIGERATION SYSTEM

Figure **1a** shows the diagram of a conventional absorption refrigeration cycle, BARC, while the compression-absorption refrigeration cycle, CARC, is illustrated in Figure **1b**. The BARC cycle operates with two pressure levels, high pressure in the generator and the condenser and low pressure in the evaporator and the absorber. The CARC cycle does it under three pressure levels, high pressure in the generator and the condenser, intermediate pressure in the absorber and low pressure in the evaporator. In reference to the BARC cycle, the liquid refrigerant coming from the condenser under high-pressure conditions (8) passes through the pre-cooler. As a result, its temperature (9) is reduced, while the vapor coming from the evaporator increases its temperature as superheating vapor (12). Subsequently, the refrigerant passes through the expansion valve reducing its temperature and pressure (10), where it is then evaporated in the evaporator (11), resulting from the heat absorbed in the refrigerated space and because of this, the cooling effect is produced. The vapor under superheating conditions (12) enters the absorber, where it is absorbed by the rich solution coming from the generator (4), through the expansion valve (6) and with it, the weak solution is formed (1), which is pumped to the generator (3) and heated in this component. The vapor produced passes to the condenser, while the solution rich in refrigerant is sent back to the absorber. To increase the energy efficiency of the absorption refrigeration system, a solution heat exchanger, SHX, is placed between the absorber and the generator. On the other hand, the CARC cycle differs from the BARC cycle, that is, the vapor refrigerant coming from the evaporator in superheating conditions (12) instead of entering directly to the absorber passes first through the compressor. This causes an increase in the temperature and the pressure of the refrigerant until it exits in (13) to go to the absorber, where it is mixed with the rich solution coming from the generator and in this way continues the cycle. It is well known that in absorption refrigeration systems using the NH_3-H_2O as working pair, it is necessary to use a rectifier to separate a small amount of water that evaporates with the refrigerant coming from the generator. However, in this study, it is considered that the vapor refrigerant at the outlet of the generator is completely ammonia for

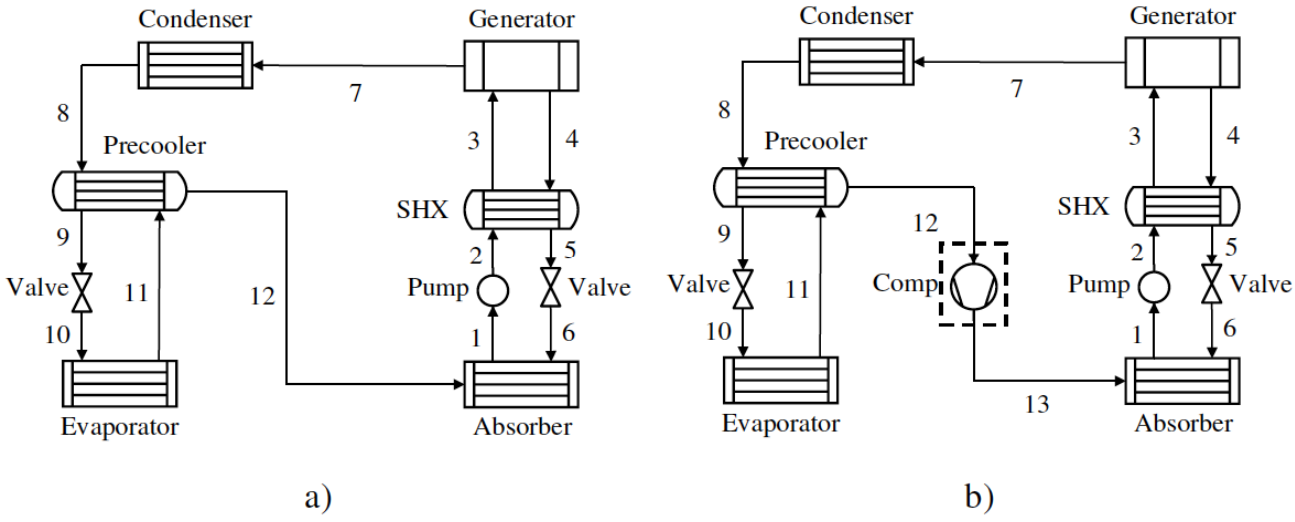

Figure 1: Refrigeration cycle **a**) simple (BARC) and **b**) with compressor (CARC).

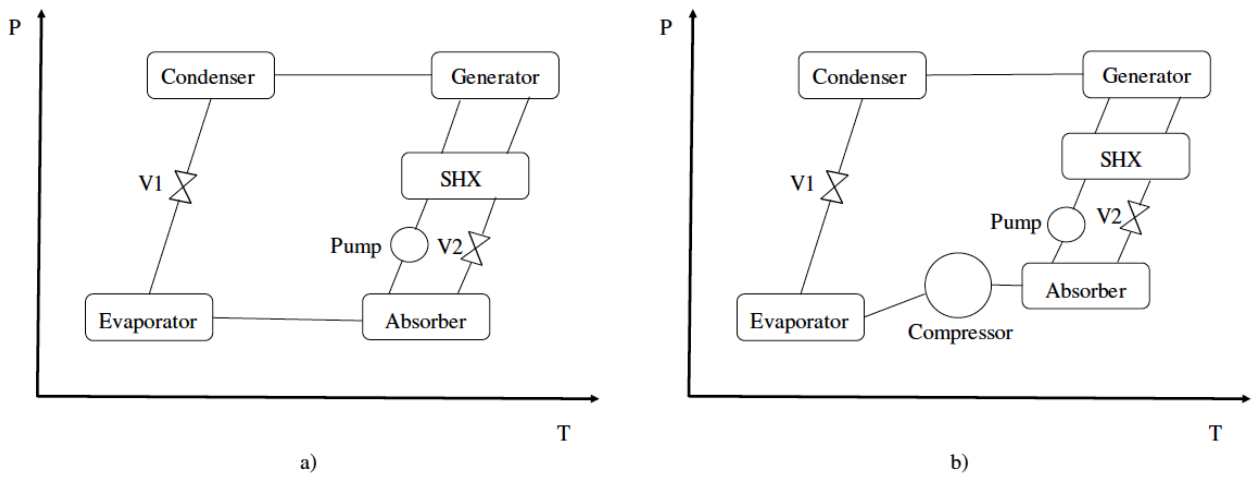

Figure 2: *P-T* diagram for absorption cycles: **a**) BARC and **b**) CARC.

compatibility with the results obtained for the cycles that operate with the three working pairs analyzed.

Figure **2** shows the *P-T* schematic diagram where the operating conditions of both systems are included. In Figure **2a**, the evaporator and absorber operate a lower pressure than the condenser and generator, while in Figure **2b**, the CARC cycle operates at three pressure levels. Low pressure in the evaporator, high pressure at the condenser and generator and the absorber operates a higher pressure than the evaporator product of the use of the compressor.

3. MODELING OF BARC AND CARC SYSTEMS

The characteristic equations of BARC and CARC systems are modeled in the Engineering Equation Solver (EES) [17], which are based on mass and energy balances describing the different components of each system. In order to make the modeling, thermodynamic properties of NH_3-H_2O pair are obtained from EES, while for NH_3-$LiNO_3$ and NH_3-Na SCN pairs, their thermodynamic properties are calculated from the work done by Infante-Ferreira [18]. The following assumptions have been made for the modeling:

- Steady state conditions were considered for each system.
- Condenser and absorber operate at the same temperature $T_{cond.} = T_{abs}$, see [8].
- The refrigerant at the condenser and the evaporator outlet is in saturation conditions.
- The refrigerant at the outlet of the generator is considered as vapor refrigerant.
- For the compatibility in the analysis for the three working pairs, the rectifier was not considered in the study of NH_3-H_2O cycle.
- There are no pressure drops in the heat exchangers neither in the pipes, it is because the effect of the internal fluid for each mixture not was considered in the analysis.
- The discharge pressure in the compressor is the same as in the absorber.

The main equations for characterizing each of the components of BARC and CARC cycles are described below (according to Figure **1**):

Generator

$$m_3 = m_4 + m_7 \tag{1}$$

$$m_3 x_3 = m_4 x_4 + m_7 \tag{2}$$

$$Q_{gen} + m_3 h_3 = m_7 h_7 + m_4 h_4 \tag{3}$$

Condenser

$$Q_{cond} = m_7 (h_7 - h_8) \tag{4}$$

Precooler

$$m_7 (h_{12} - h_{11}) = m_7 (h_8 - h_9) \tag{5}$$

$$\eta_{pres} = \frac{T_{12} - T_{11}}{T_8 - T_{11}} \tag{6}$$

Evaporator

$$Q_{evap} = m_7 (h_{11} - h_{10}) \tag{7}$$

Compressor

$$\eta_{comp} = \frac{(h_{13s} - h_{12})}{(h_{13} - h_{12})} \tag{8}$$

Where, the compressor isentropic efficiency is calculated by the equation presented by Rodríguez-Muñoz *et al*. [19], which is used for a scroll compressor type:

$$\eta_{comp} = 0.874 - 0.0135rp \tag{9}$$

While, *rp* is the compressor pressure ratio, i.e., the discharge pressure with respect to the suction pressure, which is calculated as:

$$rp = \frac{P_{abs}}{P_{evap}} \tag{10}$$

Absorber

$$m_7 h_{12} + m_6 h_6 = m_1 h_1 + Q_{abs} \tag{11}$$

In the case of CARC system, the energy balance in the absorber is calculated by:

$$m_7 h_{13} + m_6 h_6 = m_1 h_1 + Q_{abs} \tag{12}$$

Pump

$$W_{pump} = m_1 \upsilon_1 \frac{(P_2 - P_1)}{\eta_{pump}} \tag{13}$$

SHX

$$m_2(h_3 - h_2) = m_4(h_4 - h_5) \tag{14}$$

$$\eta_{SHX} = \frac{T_4 - T_5}{T_4 - T_2} \tag{15}$$

Energetic performance of an absorption refrigeration system is defined as follows:

$$COP = \frac{Q_{evap}}{\frac{Q_{gen}}{\eta_{the}} + \frac{W_{pump}}{\eta_{elect}}} \tag{16}$$

In other hand, for the CARC system, the energetic performance is obtained by the following equation:

$$COP = \frac{Q_{evap}}{\frac{Q_{gen}}{\eta_{the}} + \frac{W_{comp} + W_{pump}}{\eta_{elect}}} \tag{17}$$

Also, the exergetic efficiency for the BARC system, is defined by:

$$\eta_{ex} = \frac{Q_{evap}\left(\frac{T_0}{T_{evap}} - 1\right)}{Q_{gen}\left(1 - \frac{T_0}{T_{gen}}\right) + \frac{W_{pump}}{\eta_{elect}}} \tag{18}$$

For the CARC system, the exergetic efficiency can be obtained by:

$$\eta_{ex} = \frac{Q_{evap}\left(\frac{T_0}{T_{evap}} - 1\right)}{Q_{gen}\left(1 - \frac{T_0}{T_{gen}}\right) + \frac{W_{comp} + W_{pump}}{\eta_{elect}}} \tag{19}$$

In order to make the simulation of the absorption refrigeration system in more realistic way, in Equations (16-19) the efficiency of electricity production and electricity transmission efficiency were incorporated, where, for this paper, the values of these parameters were considered 0.38 [16] and 0.9 [20], respectively.

4. RESULTS AND DISCUSSION

This section shows the main energetic and exergetic comparisons of the compression-absorption refrigeration cycle using NH_3-H_2O, NH_3-$LiNO_3$ and NH_3-NaSCN as working pairs. The results presented are compared with those obtained from the conventional absorption refrigeration system. The simulation was performed under the same operating conditions and considering a nominal cooling capacity of 17 kW [21].

4.1. Generation Temperature

The generation temperature is an important parameter to establish the type of heat input necessary to drive the absorption refrigeration system. To know these temperatures, a simulation of the BARC and CARC cycles was performed based on equations 1-19. For the simulation, the operating parameters of the BARC cycle were considered based on the work presented by Sun [22]. These parameters are: T_{evap} = -5°C, T_{cond} = T_c= T_{abs} = 25°C and an effectiveness in the solution heat exchanger of 0.8. In addition, the effectiveness in the pre-cooler and solution pump 0.8 and 0.85, respectively, which are typical values considered in this kind of systems. Regarding the simulation of the CARC cycle, the same operating conditions of the BARC cycle were considered, as well

as variations in the compressor pressure ratio of 1.2, 1.4, 1.6, 1.8 and 2.0.

In addition to the validation of the model, the results obtained for the CARC cycle were validated with data reported by Ventas *et al*. [16] at condensation and evaporation temperature of 39°C and 0°C, respectively and *rp*=1.4. Figure **3** shows the values of COP for different generation temperatures, which indicate a good agreement between both results.

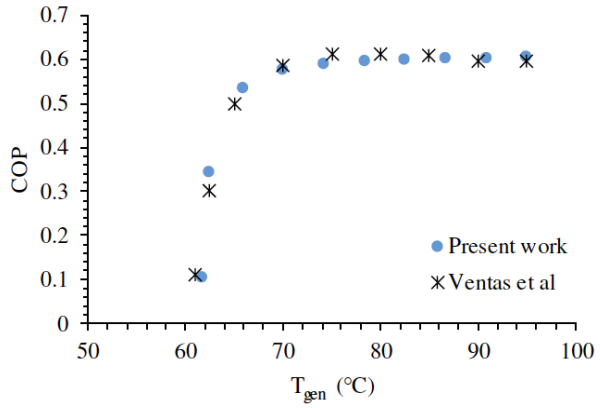

Figure 3: Validation of developed model for CARC with NH_3-$LiNO_3$ as working fluid.

In order to have a wide point of view of the generation temperatures for the three working pairs under study in this work, four conditions of condensation temperatures (=T_{abs}) of 25-40°C have been established in intervals of 5°C [23], which are commonly found in Mexico for warm climate applications. The results obtained from the simulation are shown in Table **1**.

In Table **1** it can be seen that, for the conventional absorption refrigeration cycle (BARC, *rp*=1.0) and for a condensation temperature of 25°C, the pair with the lowest generation temperature is NH_3-$LiNO_3$ (56.75°C), followed by NH_3-H_2O (59.48°C) and finally NH3-NaSCN (60.76°C). It can be observed that this trend is repeated for the different condensation temperatures, although the generation temperature is higher with respect to each pair. This is because when the cooling capacity is taken as a constant, the increase in the condensation temperature causes that a higher energy to be supplied to the generator, increasing its generation temperature. It should be noted that the lowest generation temperatures are achieved for a condensation temperature of 25°C.

On the other hand, the increasing the compressor pressure ratio in the CARC cycle contributes to a reduction in the generation temperature for the three working pairs and this reduction is lower when the condensation temperature decreases. For example, for a *rp*=2.0 and a condensation temperature of 25°C, the reductions that are obtained in the generation temperature compared with the basic refrigeration cycle (BARC, *rp*=1.0), are 22.86°C for NH_3-H_2O, 20.88°C for NH_3-$LiNO_3$ and 23.76°C with NH_3-NaSCN. For a condensation temperature of 40°C, these reductions are 24.99°C, 21.97°C and 26.21°C, respectively.

4.2. Energetic Analysis

This section presents the behavior of COP for both absorption refrigeration cycles when parameters such

Table 1: Generation Temperatures for the Three Working Pairs Analyzed in this Work

Cycle	Generation temperatures (°C)											
	T_{cond}=T_{abs}=25°C			T_{cond}=T_{abs}=30°C			T_{cond}=T_{abs}=35°C			T_{cond}=T_{abs}=40°C		
	NH_3-H_2O	NH_3-$LiNO_3$	NH_3-NaSCN	NH_3-H_2O	NH_3-$LiNO_3$	NH_3-NaSCN	NH_3-H_2O	NH_3-$LiNO_3$	NH_3-NaSCN	NH_3-H_2O	NH_3-$LiNO_3$	NH_3-NaSCN
BARC (*rp*=1.0)	59.48	56.75	60.76	70.92	67.29	72.35	82.58	77.88	84.16	94.48	88.52	96.10
CARC (*rp*=1.2)	53.57	51.36	54.52	64.85	61.82	65.90	76.32	72.33	77.46	88.02	82.87	89.22
CARC (*rp*=1.4)	48.51	46.75	49.23	59.64	57.12	60.45	70.96	67.55	71.82	82.52	78.02	83.42
CARC (*rp*=1.6)	44.09	42.71	44.65	55.08	52.99	55.71	66.28	63.36	66.94	77.70	73.78	78.34
CARC (*rp*=1.8)	40.16	39.12	40.60	51.02	49.33	51.52	62.09	59.62	62.62	73.37	69.98	73.90
CARC (*rp*=2.0)	36.62	35.87	37.00	47.36	46.02	47.78	58.32	56.25	58.75	69.49	66.55	69.89

as: generation temperature, condensation and evaporation temperature, as well as the compressor pressure ratio are varying. In this sense, Figure **4** illustrates the influence of the generation temperature, T_{gen}, on the COP of the systems for the three working pairs. In addition, the behavior of the COP for the four condensation temperature conditions is also illustrated. Additionally, the effect of the compressor pressure ratio is shown through the different figures.

Figure **4a** depicts COP of the BARC refrigeration system (*rp*=1.0) as a function of generation temperature. It is seen that the COPs are obtained using the NH_3-$LiNO_3$ pair for most of the range of generation and condensation temperatures. This behavior is more marked for condensation temperatures of 35°C and 40°C, where even for these same operating conditions, the COPs for the NH_3-H_2O and NH_3-NaSCN pairs are very similar. On the other hand, Figures **4b-f** show the COP for the CARC cycle, where the influence of the compressor pressure ratio for the three working pairs is analyzed. As the compressor pressure ratio increases, it is observed that the difference between COPs for the three working pairs is getting smaller, and this is more noticeable at lower condensation temperatures. However, at a compression ratio of 2.0 (Figure **4f**), the NH_3-H_2O pair shows COPs that result to be slightly higher than the other two pairs and this is achieved for almost all range of condensation and generation temperatures. This is

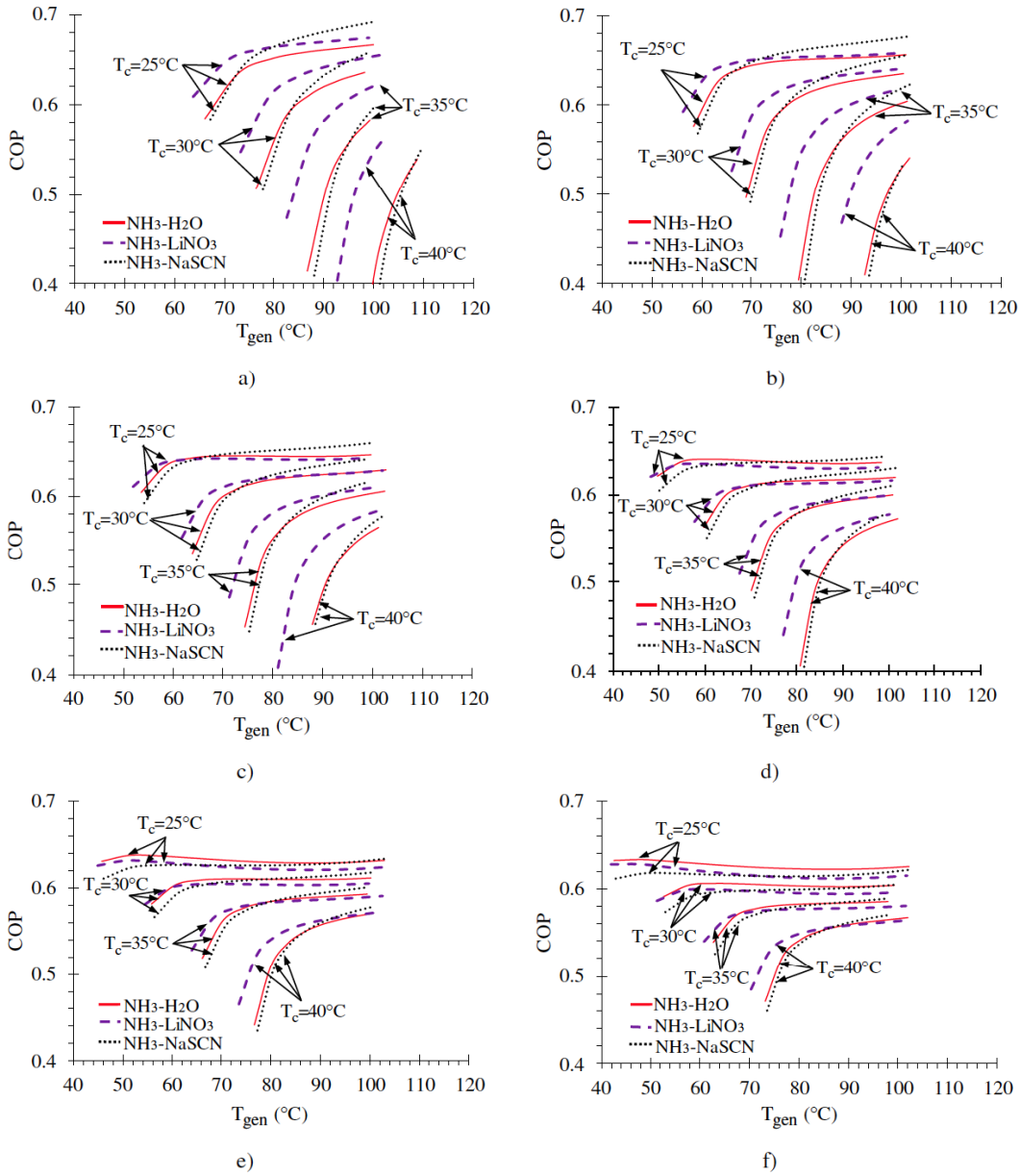

Figure 4: COP vs T_{gen} for different values of *rp*; **a**) 1.0, **b**) 1.2, **c**) 1.4, **d**) 1.6, **e**) 1.8 y **f**) 2.0.

due to the fact that increase the compressor pressure ratio, it produces a reduction in the enthalpies in the states 4 and 5, as well as less mass flow rate in the strong and weak solution and then less energy is required in the generator to begin producing the refrigerating effect. However, this reduction is significantly lower for NH_3-H_2O, which results in a better COP in the cycle.

On the other hand, Figure **5** illustrates the effect of the evaporation temperature on the COP of the BARC (see Figure **5a**) and CARC (see Figures **5b-f**) cycles for the three working pairs under study. The coefficient of performance is analyzed for the same operating conditions described in Figure **4**, in addition, a generation temperature of 90°C was set. The results show that the COP increases as the evaporation temperature increases, while it decreases as the condensation temperature increases. Figure **5a** it is also seen that the COPs are very similar for the three working pairs at a condensation temperature of 25°C and 30°C, with the NH_3-NaSCN pair being slightly higher than the other two pairs. At condensation temperatures of 35°C and 40°C, the difference on COPs between pairs is more remarkable, so for these operating conditions NH_3-$LiNO_3$ pair is higher than the other two pairs for practically all the range of evaporation temperatures. Figure **3b** shows COP is similar to those obtained in the case of Figure **5a**. The NH_3-NaSCN is slightly higher than the other pairs and

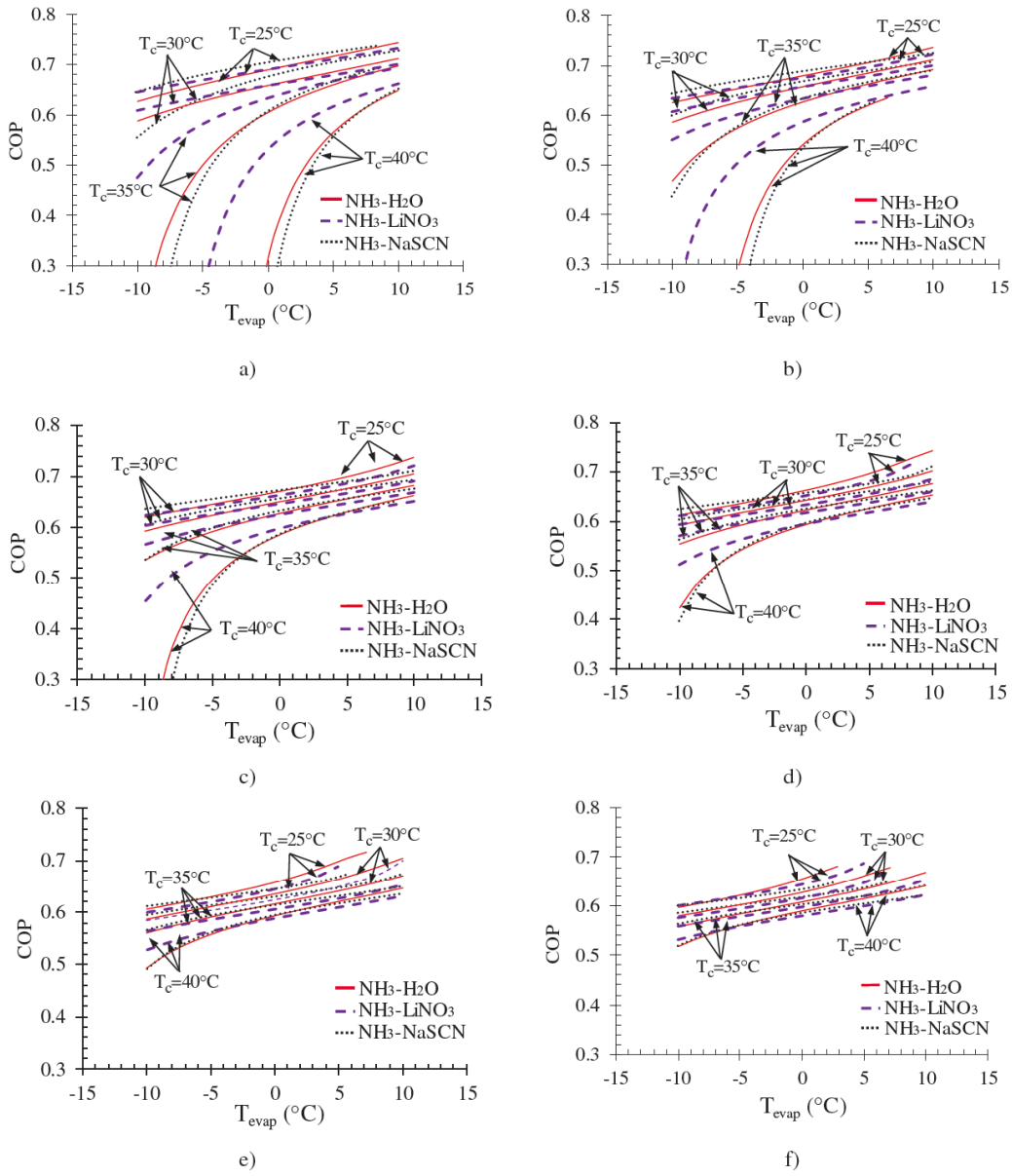

Figure 5: COP vs T_{evap} for different values of *rp*; **a**) 1.0, **b**) 1.2, **c**) 1.4, **d**) 1.6, **e**) 1.8 y f) 2.0.

the best results are obtained at low condensation temperatures. On the other hand, it can also be observed that NH_3-$LiNO_3$ has a higher COP than NH_3-H_2O and NH_3-NaSCN for almost all the range of evaporation temperatures, however this is obtained at a condensation temperature of 40°C. In the case of the cycle operating at *rp*=1.4 and 1.6 (Figures **5c** and **5d**), NH_3-H_2O begins to be higher than the other two pairs at evaporation temperatures above 0°C. It is important to indicate that, as the compressor pressure ratio increases, as well as the evaporation temperature, the difference between energetic behavior among pairs become smaller each time. When the cycle works at *rp*= 1.8 and 2.0 (Figures **5e** and **5f**), it is observed that there are not many variations on the energetic behavior among pairs. However, at condensation temperature of 25°C, it can be seen that the NH_3-H_2O pair shows COPs are slightly higher than those obtained from the other two pairs, although this is achieved at evaporation temperatures higher than -7°C. This is mainly due to two aspects; by increasing the evaporation temperature, the energy consumption of the compressor is reduced, while the increasing in the compressor pressure ratio causes a reduction in the generation temperature for the three pairs, work of the solution pump and the mass flow rate coming from generator. However, in the case of the NH_3-H_2O cycle, this effect is more beneficial in comparison with the other working pairs and, therefore, better COPs are obtained.

4.3. Exergetic Analysis

Figure **6** shows the exergetic efficiency of the absorption refrigeration system as a function of the generation temperature, condensation temperature and compressor pressure ratio. For the simulation, the reference state was taken at an ambient temperature of 25°C, a pressure of 101.325kPa and an evaporation temperature of -5°C. From the results obtained it is observed that the exergetic efficiency, η_{ex}, reaches a maximum point at a specific generation temperature for each condenser temperature, however after of its value, the energetic efficiency decreases while the generation temperature increases. This phenomenon is because increasing the generation temperature causes a significant increase in the absorption efficiency of the solution, increasing with it the absorption rate of the weak solution into the strong solution and then, a lower energy is required in the generator. In addition, it is also observed that an increase in the condensation temperature causes a decrease in the exergetic efficiency for the three working pairs. This is because, as the condensation temperature increases, the energy required in the generator increases, so that, by definition of the second law of thermodynamics (Equations (18) and (19)), increases the exergy supplied and thereby, reducing the exergetic efficiency.

In the case of Figure **6a** (BARC cycle, *rp* = 1.0), the NH_3-$LiNO_3$ pair has better exergetic efficiency for a wide range of generation and condensation temperatures, and these results are more noticeable at high condensation temperatures. With respect to the NH_3-H_2O and NH_3-NaSCN pairs, it is observed that both exergetic efficiencies are very similar for low and high generation and condensation temperatures. On the other hand, Figures **6b-f** illustrate that, by increasing the compression ratio, the exergetic efficiency of the CARC cycle is reduced and, in turn, a lower generation temperature is achieved. It is also observed that the exergetic efficiencies are very similar for the three working pairs, for the whole range of generation and condensation temperatures, even the difference of the η_{ex} is reduced as the compressor pressure ratio increases.

The effects of the evaporation and condensation temperature on the exergetic efficiency are shown in Figure **7**. For the analysis, a generation temperature of 90°C was considered, which was kept constant during the simulation. From the figure it is observed that, under the same operating conditions, the exergetic efficiency for the three working pairs is drastically reduced when the evaporation and condensation temperature is increased. When the refrigeration system operates at low evaporation temperatures, more energy is required in the generator to produce the cooling process. For example, this effect is most noticeable at high condensation temperatures (35°C and 40°C) as is shown in Figures **7a-c**. However, the increase in evaporation temperature causes a reduction in the input exergy more widely than the output exergy, which causes that the exergy efficiency to increase to its optimum value. From this value, the exergetic efficiency begins to decrease because there are not many variations in the output exergy, while the input exergy continues reducing significantly.

The best results correspond to a condensation temperature of 25°C and 30°C, as well as to low evaporation temperatures (see Figure **7a**). Figure **5a** also shows that at condensation temperature of 35°C, NH_3-$LiNO_3$ is higher than the other two pairs, but this is achieved at evaporation temperatures below 3°C, while at condensation temperature of 40°C, this pair is higher

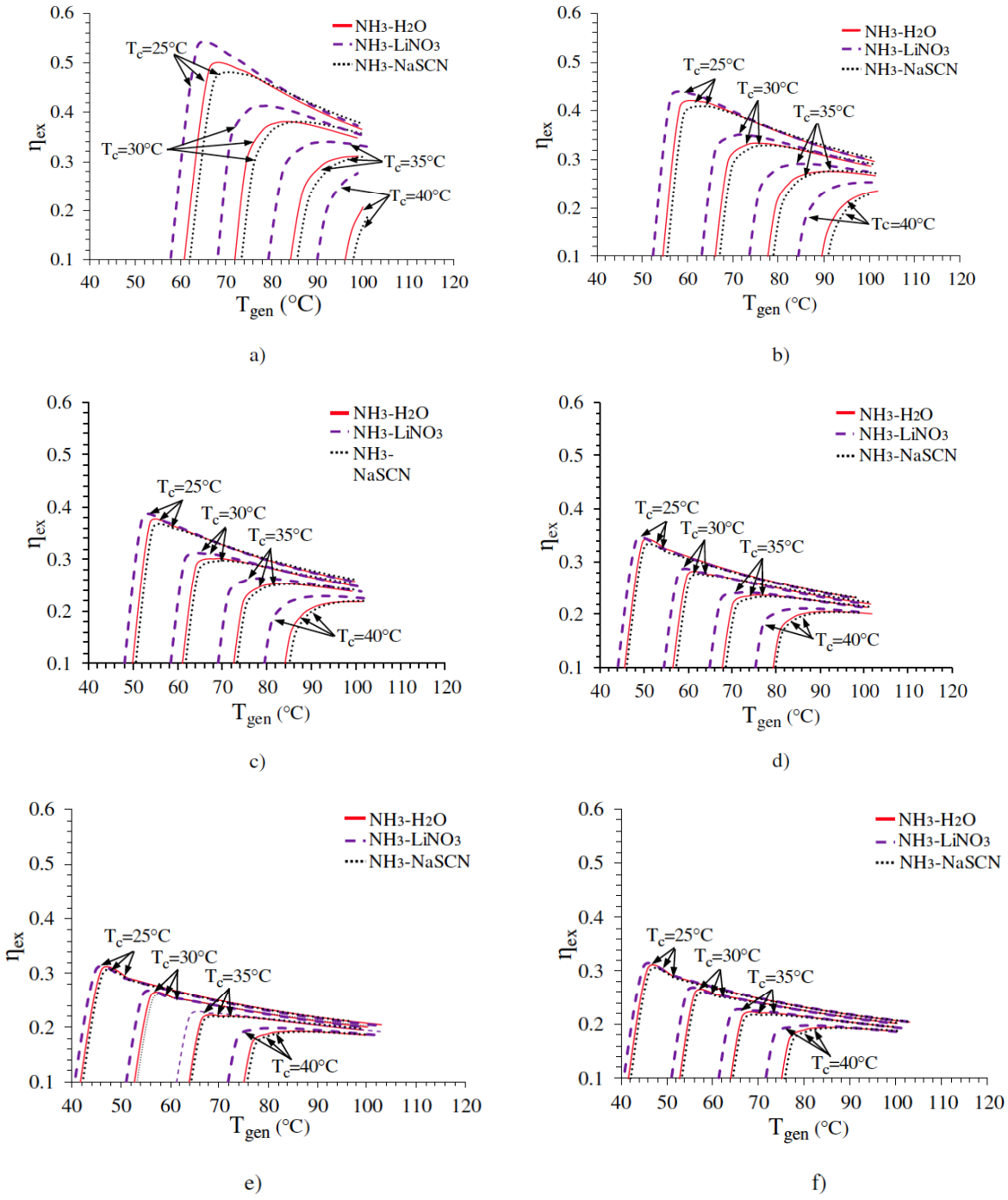

Figure 6: η_{ex} vs T_{gen} for different values of *rp*; **a**) 1.0, **b**) 1.2, **c**) 1.4, **d**) 1.6, **e**) 1.8 y **f**) 2.0.

than the other two for almost all of range of evaporation temperatures. In Figures **7b** and **7c** it is observed that when compressor pressure ratio increases, the difference between exergy behaviors is reduced and this reduction is less at low condensation temperatures. For example, at a *rp* = 1.2 and 1.4, as well as a condensation temperature of 35°C, the NH_3-$LiNO_3$ is still higher than the other two pairs, but this is achieved at evaporation temperatures lower than 0°C and -5°C, respectively. Considering the same compressor pressure ratio and a condensation temperature of 40°C, this working pair is still slightly higher than the other two pairs, however, its exergetic efficiency decrease with the increase of the compressor pressure ratio.

For a *rp*=1.6 (see Figure **7d**), it can be seen that, practically, the energetic behaviors are very similar for the three working pairs, for both low and high condensation temperatures and this same effect is

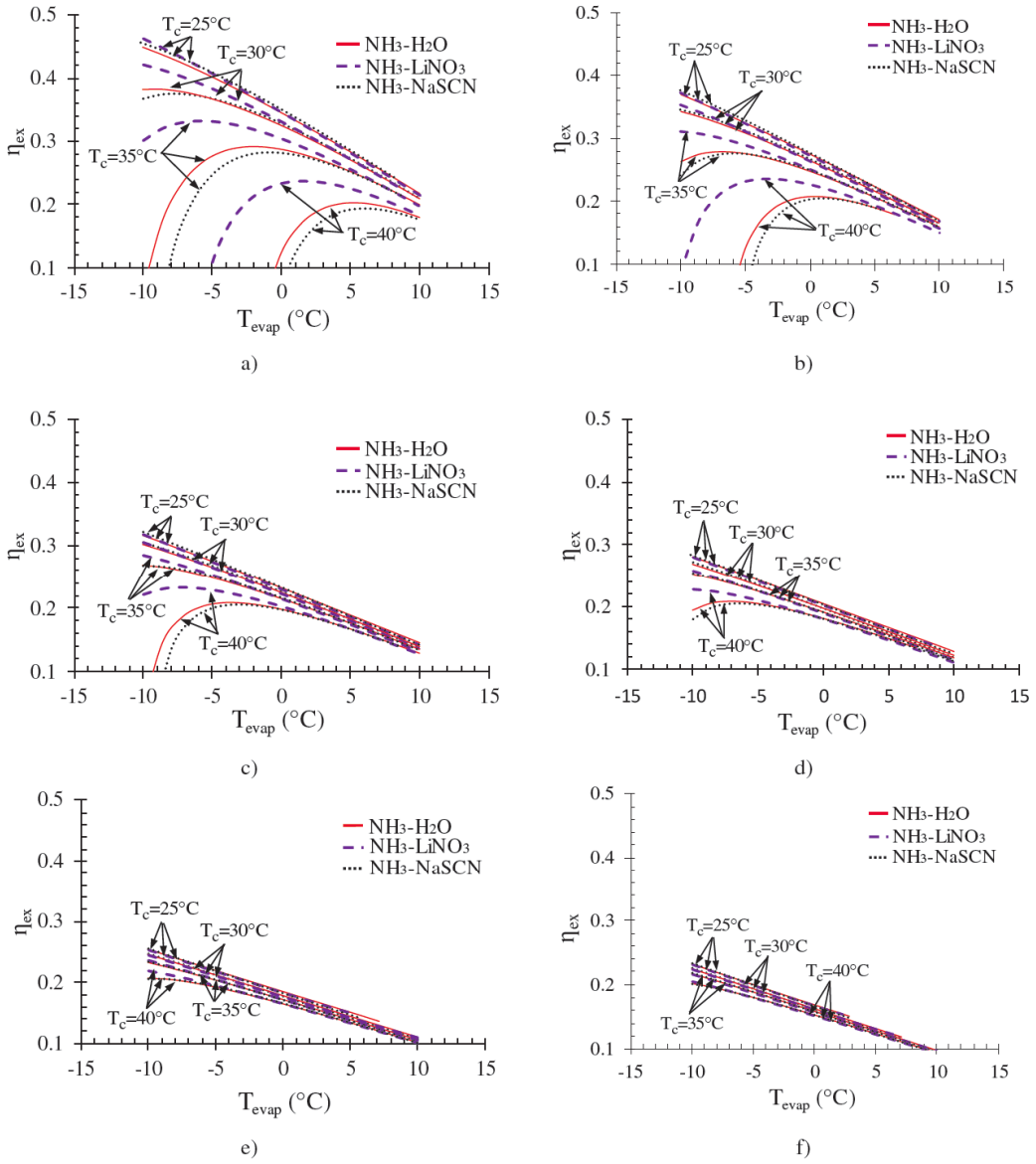

Figure 7: η_{ex} vs T_{evap} for different values of *rp*; **a**) 1.0, **b**) 1.2, **c**) 1.4, **d**) 1.6, **e**) 1.8 y f) 2.0.

more noticeable for a *rp*=1.8 and 2.0. However, for low condensation temperatures, the CARC cycle is more suitable for refrigeration applications.

5. CONCLUSIONS

In this paper, the energetic and exergetic comparison of a compression-absorption refrigeration system was presented, in which three working pairs were evaluated. The parameters analyzed were generation temperature, evaporation temperature, condensation temperature and compressor pressure ratio, and the results obtained were compared with those obtained by the basic absorption refrigeration cycle. Among the most relevant conclusions of this work we can mention the following:

- The compressor pressure ratio is the parameter that shows a higher influence on the coefficient of performance of the CARC cycle for the three working pairs studied. The NH_3-H_2O pair presents a slight increase on COP compared to the other two pairs at high compressor pressure ratio (*rp*>1.8), as well at low condensation temperatures. For example, for a *rp*=2.0 and a condensation temperature of 25°C, the reductions on the generation temperature obtained in comparison with the basic refrigeration cycle (BARC), are 22.86°C with NH_3-H_2O, of 20.88°C for NH_3-$LiNO_3$ and 23.76°C with NH_3-NaSCN, while a condensation temperature of 40°C, these reductions are 24.99°C, 21.97°C and 26.21°C respectively.

- By increasing the compressor pressure ratio, the exergetic efficiency of the CARC cycle decreases for the three working pairs. However, similar energetic performances are found for the three working pairs at high range of generation and condensation temperatures.

- Increasing the evaporation temperature causes energetic efficiency to increase while the exergetic efficiency is reduced. From the energetic point of view, the NH_3-H_2O results are slightly higher than for the other two working pairs at high compressor pressure ratio, high evaporation temperatures, as well at low condensation temperatures. While for these same operating conditions, the exergetic efficiency for the three working pairs are very similar.

- The CARC cycle is a good alternative for solar energy applications since generation temperatures between 35-37°C are necessary to activate the system for the three working pairs at condensation temperatures of 25°C.

- The results show that energetic and exergetic performances are lower for NH_3-H_2O compared with the other two working pairs when used in the BARC cycle. However, when implementing this pair in the CARC cycle, these results are beneficial since the energetic and exergetic performances are similar to the other pairs, and even for even operating conditions, the NH_3-H_2O is slightly higher than the other two.

- The use of NH_3-H_2O has the advantage of no crystallization risk as in the case of NH_3-$LiNO_3$ and NH_3-NaSCN pairs. It is because when the system works with NH_3-$LiNO_3$ and NH_3-NaSCN and the generation temperature increasing while remaining constant the condensation temperature, the mixture tends to enter the crystallization zone because the weak solution coming to the generator decreases.

- With the results, it is expected that this work helps the researchers and designers to search energetic improvements on this type of system and in the developing of new alternative configurations of absorption-compression refrigeration systems and development of new compressors able operate under the operating conditions of maximum COP and exergetic efficiency.

Finally, the present study allows us to conclude that the CARC cycle is an alternative configuration for absorption refrigeration systems in the field of refrigeration and air conditioning, since the generation temperature can be reduced up 26.21°C, compared with the basic absorption refrigeration cycle (BARC). In addition, it also shows that in the CARC configuration, the NH_3-H_2O mixture results in COP and energetic efficiency competitive compared with NH_3-NaSCN and NH_3-$LiNO_3$ mixture.

ACKNOWLEDGEMENTS

The authors wish to thank the University of SABES and University of Guanajuato by the support in the realization of this article.

NOMENCLATURE

h = enthalpy (kJ/kg)

m = mass flow rate (kg/s)

P = pressure (kPa)

Q = heat transfer rate (kW)

T = temperature (°C)

V = Valve

SHX = Solution heat exchanger

u = specific volume (m^3/kg)

W = power (kW)

x = ammonia-solution concentration

Subscripts

abs = absorber

comp = compressor

cond = condenser

elect = electricity

evap = evaporator

ex = exergetic

gen = generator

prec = precooler

pump = pump

s = isentropic

SHX = solution heat exchanger

the = thermal

0,1, 2,… = thermodynamic states

REFERENCES

[1] She X, Cong L, Nie B, Leng G, Peng H, Chen Y, Zhang X, Wen T, Yang H, Luo Y. Energy-efficient and-economic technologies for air conditioning with vapor compression refrigeration: A comprehensive review. Applied Energy 2018; 232: 157-86. https://doi.org/10.1016/j.apenergy.2018.09.067

[2] Kalinowski P, Hwang Y, Radermacher R, Al Hashimi S, Rodgers P. Application of waste heat powered absorption refrigeration system to the LNG recovery process. International journal of refrigeration 2009; 32(4): 687-94. https://doi.org/10.1016/j.ijrefrig.2009.01.029

[3] Xu ZY, Mao HC, Liu DS, Wang RZ. Waste heat recovery of power plant with large scale serial absorption heat pumps. Energy 2018; 165: 1097-105. https://doi.org/10.1016/j.energy.2018.10.052

[4] Jing Y, Li Z, Liu L, Lu S. Exergoeconomic Assessment of Solar Absorption and Absorption–Compression Hybrid Refrigeration in Building Cooling. Entropy 2018; 20(2): 130. https://doi.org/10.3390/e20020130

[5] Zhu L, Gu J. Second law-based thermodynamic analysis of ammonia/sodium thiocyanate absorption system. Renewable Energy 2010; 35(9): 1940-6. https://doi.org/10.1016/j.renene.2010.01.022

[6] Cai D, He G, Tian Q, Tang W. Exergy analysis of a novel air-cooled non-adiabatic absorption refrigeration cycle with NH3–NaSCN and NH3–LiNO3 refrigerant solutions. Energy Conversion and Management 2014; 88: 66-78. https://doi.org/10.1016/j.enconman.2014.08.025

[7] Cai D, Jiang J, He G, Li K, Niu L, Xiao R. Experimental evaluation on thermal performance of an air-cooled absorption refrigeration cycle with NH3–LiNO3 and NH3–NaSCN refrigerant solutions. Energy Conversion and Management 2016; 120: 32-43. https://doi.org/10.1016/j.enconman.2016.04.089

[8] Farshi LG, Ferreira CI, Mahmoudi SS, Rosen MA. First and second law analysis of ammonia/salt absorption refrigeration systems. International Journal of Refrigeration 2014; 40: 111-21. https://doi.org/10.1016/j.ijrefrig.2013.11.006

[9] Morawetz E. Sorption-compression heat pumps. International journal of Energy Research 1989; 13(1): 83-102. https://doi.org/10.1002/er.4440130109

[10] Wang J, Wang B, Wu W, Li X, Shi W. Performance analysis of an absorption-compression hybrid refrigeration system recovering condensation heat for generation. Applied Thermal Engineering 2016; 108: 54-65. https://doi.org/10.1016/j.applthermaleng.2016.07.100

[11] Wu W, Shi W, Wang J, Wang B, Li X. Experimental investigation on NH3–H2O compression-assisted absorption heat pump (CAHP) for low temperature heating under lower driving sources. Applied Energy 2016; 176: 258-71. https://doi.org/10.1016/j.apenergy.2016.04.115

[12] Ahmadi P, Rezaie B. Work availability and exergy analysis. Entropy 2018; 20: 597. https://doi.org/10.3390/e20080597

[13] Ayou DS, Bruno JC, Coronas A. Integration of a mechanical and thermal compressor booster in combined absorption power and refrigeration cycles. Energy 2017; 135: 327-41. https://doi.org/10.1016/j.energy.2017.06.148

[14] Takleh HR, Zare V. Employing thermoelectric generator and booster compressor for performance improvement of a geothermal driven combined power and ejector-refrigeration cycle. Energy Conversion and Management 2019; 186: 120-30. https://doi.org/10.1016/j.enconman.2019.02.047

[15] Razmi A, Soltani M, Kashkooli F, Farshi LG. Energy and exergy of an enviorenmentally-friendly hybrid absorption/ recompression refrigeration system. Energy Conversion and Management 2018; 164: 59-69. https://doi.org/10.1016/j.enconman.2018.02.084

[16] Ventas R, Lecuona A, Zacarías A, Venegas M. Ammonia-lithium nitrate absorption chiller with an integrated low-pressure compression booster cycle for low driving temperatures. Applied Thermal Engineering 2010; 30(11-12): 1351-9. https://doi.org/10.1016/j.applthermaleng.2010.02.022

[17] Klein SA. Engineering Equation Solver 2015, V9.911 F-Chart Software.

[18] Ferreira CI. Thermodynamic and physical property data equations for ammonia-lithium nitrate and ammonia-sodium thiocyanate solutions. Solar Energy 1984; 32(2): 231-6. https://doi.org/10.1016/S0038-092X(84)80040-7

[19] Rodríguez-Muñoz JL, Pérez-García V, Belman-Flores JM, Ituna-Yudonago, J.F. Energy and exergy performance of the IHX position in ejector expansion refrigeration systems. Int J Refrig 2018; 93: 122-131. https://doi.org/10.1016/j.ijrefrig.2018.06.017

[20] Gazda W, Kozioł J. The estimation of energy efficiency for hybrid refrigeration system. Applied Energy 2013; 101: 49-57. https://doi.org/10.1016/j.apenergy.2012.05.006

[21] Jacob U, Spiegel K, Pink W. Development and experimental investigation of a novel 10 kW ammonia/water absorption chiller for air conditioning and refrigeration systems. In 9th International IEA heat pump conference. Zurich, Switzerland 2008; pp. 1-8.

[22] Sun DW. Comparison of the performances of NH3-H2O, NH3-LiNO3 and NH3-NaSCN absorption refrigeration systems. Energy Conversion and Management 1998; 39(5-6): 357-68. https://doi.org/10.1016/S0196-8904(97)00027-7

[23] Purohit N, Gupta DK, Dasgupta MS. Experimental investigation of a CO2 trans-critical cycle with IHX for chiller application and its energetic and exergetic evaluation in warm climate. Applied Thermal Engineering 2018; 136: 617-32. https://doi.org/10.1016/j.applthermaleng.2018.03.044

Received on 17-11-2019 Accepted on 17-12-2019 Published on 18-12-2019

DOI: http://dx.doi.org/10.15377/2409-5826.2019.06.7